Steel and Composite Structures, *Vol. 27, No. 1* (*2018*) *35-48*
DOI: https://doi.org/10.12989/scs.2018.27.1.035

Deformation and stress analysis of a sandwich cylindrical shell using HDQ Method

Hassan Shokrollahi *

Department of Mechanical Engineering, Faculty of Engineering, Kharazmi University, Mofatteh Avenue, P.O. Box 15719-14911, Tehran, Iran

(*Received July 27, 2017, Revised January 26, 2018, Accepted January 29, 2018*)

Abstract. In this paper, the response of a sandwich cylindrical shell over any sort of boundary conditions and under a general distributed static loading is investigated. The faces and the core are made of some isotropic materials. The faces are modeled as thin cylindrical shells obeying the Kirchhoff-Love assumptions. For the core material it is assumed to be thick and the in-plane stresses are negligible. The governing equations are derived using the principle of the stationary potential energy. Using harmonic differential quadrature method (HDQM) the equations are solved for deformation components. The obtained results primarily are compared against finite element results. Then, the effects of changing different parameters on the stress and displacement components of sandwich cylindrical shells are investigated.

Keywords: sandwich cylindrical shells; harmonic differential quadrature method; static analysis; general lateral loading; general boundary conditions

1. Introduction

Sandwich shells are widely used in many engineering applications, especially in aerospace and marine industries. They commonly consist of two load carrying faces connected by usually soft inner layer (core). The faces are made of materials with high stiffnesses, as steel, aluminum alloys, reinforced plastics and the core can be made of corrugated sheet, wood, foam, rubber, etc. Generally, the sandwich shells are lightweight structures with very high stiffness to weight and strength to weight ratios and they also have very good thermal and acoustic isolation properties.

To date the study on the shell behavior is well-developed and historically is back-dated to early 40s. A summary of early works can be found in some textbooks written by Plantema (1966), Allen (1969), and Zenkert (1995). Some newer comprehensive reviews can be found in (Noor *et al.* 1996, Librescu and Hause 2000, Vinson 2001, Altenbach 2011) in which various analytical and computational models for sandwich structures are presented. Moreover, some analytical and numerical solution of shells can be found in (Ng and Lam 1999, Civalek 2007a, b, 2008a, b, Zhong and Yu 2009). In overview of these works it can be concluded that when the overall or global response of a sandwich shell is under consideration, there is no need to use complicated or high-order theories. That is an accurate prediction of the shell response can be achieved using the classical sandwich shell theory assumptions. However, in the case of sandwich structures with a soft-core highly deformable in the thickness direction, the Murakami's function is suggested to be added to the kinematic model to capture the zig-zag effect. More details about this issue can be found in (Carrera 2003, 2004, Tornabene *et al.* 2017).

Generalized differential quadrature method (GDQM) is a rather new numerical method which has been used widely in solving problems in different engineering fields (Allahkarami *et al.* 2017, Mohammadimehr and Shahedi 2016, Hamzehkolaei *et al.* 2011). The GDQM was developed by Shu and coworkers (Shu 2000, Shu and Richards 1992) based on the DQ technique (Bellman *et al.* 1972). On the other hand, the harmonic differential quadrature method (HDQM) is a fast converging version of the GDQM (Civalek 2004). In general, in all different versions of the DQ method, the partial derivative of a function, with respect to a spatial variable at a given discrete point, will be approximated by a linear summation of weighted function values at all discrete points chosen in the solution domain of the spatial variable (Shu 2000, Shu and Richards 1992). Some advantages of the DQ method in comparison with the finite element method (FEM) are the ease of its implementation on the governing equations and spending less computational efforts in solving any problem. The reason lies in the fact that in the DQ method the natural and essential boundary conditions must be satisfied simultaneously, while in FEM the natural boundary conditions are included in the weak form solution of the governing equations, and the approximate displacement functions must satisfy only the essential boundary conditions of the problem. In other words, the DQM and FEM deal with strong and weak form of governing differential equations, respectively.

A review of several applications of the numerical technique at issue, including different approaches, can be

*Corresponding author, Ph.D.,
E-mail: hshokrollahi@khu.ac.ir

http://www.techno-press.org/?journal=scs&subpage=6

ISSN: 1229-9367 (Print), 1598-6233 (Online)

found in Tornabene *et al.* (2015). Also, some studies about other solution methods of panel and shells can be found in Abouhamze *et al.* (2007) for Extended Kantorovich Method, in Civalek and Gürses (2009) for discrete singular convolution technique, in Zhao *et al.* (2004), for the mesh-free Kp-Ritz method, in (Civalek 2008a, Gürses *et al.* 2009, 2012, Baltacıoglu *et al.* 2010) for the method of discrete singular convolution, and in Bhimaraddi and Chandrashekhara (1992) for three-dimensional elasticity solution. There are some works in the literatures in which the DQM has been used in static analysis of the laminated cylindrical shell panel. For example, Maleki *et al.* (2012) used GDQM in static and transient analysis of thin/moderately thick laminated shell panels subjected to different loadings and boundary conditions. Tornabene *et al.* (2012) applied the GDQM in the static analysis of laminated composite shell panel of revolution with various lamination schemes and different layers. Malekzadeh (2009) used the DQM in the in-plane static analysis of laminated composite arches with any type of boundary conditions. On the other hand, the analytical solutions are limited to the type of boundary conditions. For example, Alankaya and Oktem (2016) used an analytical method for the problem of static analysis of cross-ply doubly-curved shells with the mixed type simply supported boundary conditions prescribed on the edges.

To the best knowledge of the author, reported works in the literatures were only for the case of fully simply supported sandwich shells, in which exact closed-form solutions are presented using Fourier series. The aim of present work is to study the behavior of cylindrical sandwich shells with any sort of boundary conditions under a generally distributed static loading using HDQM. The obtained results are compared with finite element results. As a result, one can find that if an accurate prediction of the shell overall response can be achieved using the classical sandwich shell theory assumptions. Then, the effects of changing different parameters on the stress and displacement components of sandwich cylindrical shells are investigated.

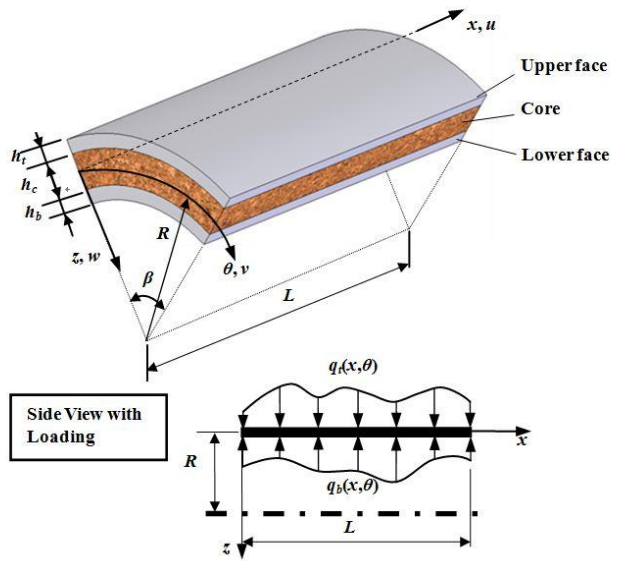

Fig. 1 Geometry of the sandwich cylindrical shell and applied loading

2. Problem definition and assumptions

Fig. 1 shows an open sandwich cylindrical shell with general boundary conditions subjected to arbitrary lateral loadings (as a function of x and θ) imposed simultaneously at inner and outer surfaces. It is assumed that the loads are exerted in a rather quasi-static manner. The displacement components corresponding to the x (longitudinal), θ (circumferential) and z (radial) directions are represented by u, v and w, respectively. According to Fig. 1, β represents the subtended angle, R is the radii of curvature of the core mid-plane, L is the length of the shell, h_t, h_c and h_b are the upper face, core and lower face thicknesses, respectively. The faces and the core are assumed to be made of isotropic materials. The faces are modeled as thin cylindrical shells and analyzed based on the classical Love's shell theory. The core material is assumed to be thick and its in-plane stresses are negligible. The core and the faces are perfectly bonded that is no delamination will occur in the core/face interfaces. Also, following assumptions prevailing in the macro-mechanical modeling of the sandwich structures are used (Altenbach *et al.* 2004):

- The thickness of the core is much greater than the thicknesses of faces, i.e. h_t, $h_b << h_c$.
- The out-of-plane transverse shear stresses, $\tau_{\theta z}$ and τ_{xz}, are neglected within the faces.
- The core only transmits shear stresses, $\tau_{\theta z}$ and τ_{xz}, and its other stress components i.e. σ_x, σ_θ, $\tau_{x\theta}$ and σ_z are negligible.

3. Formulation

3.1 Strain displacement relations

Referred to Fig. 1, the displacement components u_t, v_t, and w_t of an arbitrary point located on the domain contributed to the upper face i.e., $-h_c/2-h_t \le z \le -h_c/2$ are as follows (Jaskula and Zielnica 2011)

$$u_t(x,\theta,z) = u_1(x,\theta) + \left(z + \frac{h_c + h_t}{2}\right)\frac{\partial w_1(x,\theta)}{\partial x} \quad (1a)$$

$$v_t(x,\theta,z) = v_1(x,\theta) + \left(z + \frac{h_c + h_t}{2}\right)\frac{1}{R_t}\frac{\partial w_1(x,\theta)}{\partial \theta} \quad (1b)$$

$$w_t(x,\theta,z) = w_1(x,\theta) \quad (1c)$$

where $R_t = R + (h_c + h_t) / 2$ and, u_1, v_1 and w_1 are the displacements of an arbitrary point located on mid-surface of the upper face in x, θ and z directions, respectively. Also the displacement components u_b, v_b and w_b of an arbitrary point located on the domain contributed to any point on the lower face i.e., $h_c / 2 \le z \le h_c / 2 + h_b$ are as follows (Jaskula and Zielnica 2011)

$$u_b(x,\theta,z) = u_2(x,\theta) + \left(z - \frac{h_c + h_b}{2}\right)\frac{\partial w_2(x,\theta)}{\partial x} \quad (2a)$$

$$v_b(x,\theta,z) = v_2(x,\theta) + \left(z - \frac{h_c + h_b}{2}\right)\frac{1}{R_b}\frac{\partial w_1(x,\theta)}{\partial \theta} \quad (2b)$$

$$w_b(x,\theta,z) = w_2(x,\theta) \quad (2c)$$

where $R_b = R - (h_c + h_t) / 2$ and, u_2, v_2 and w_2 are the displacements of an arbitrary point located on mid-surface of the lower face in x, θ and z directions, respectively.

It is further assumed that at a specific section, any neighbouring point between the core and faces undergo similar transverse displacements throughout the thickness (z) direction during the deformation. In other words, $w_c(x, \theta, z) = w_t(x, \theta, z) = w_b(x, \theta, z) = w(x, \theta)$ at each cross-section.

The displacement components, u_c, v_c and w_c of an arbitrary point located on domain contributed to the core section i.e., $-h_c/2 \le z \le h_c/2$ are as follows (Jaskula and Zielnica 2011)

$$\begin{aligned} u_c(x,\theta,z) &= \frac{u_1(x,\theta)+u_2(x,\theta)}{2} + \frac{h_t - h_b}{4}\frac{\partial w(x,\theta)}{\partial x} \\ &+ \frac{2z}{h_c}\left(\frac{u_1(x,\theta)-u_2(x,\theta)}{2} + \frac{h_t + h_b}{4}\frac{\partial w(x,\theta)}{\partial x}\right) \end{aligned} \quad (3a)$$

$$\begin{aligned} v_c(x,\theta,z) &= \frac{v_1(x,\theta)+v_2(x,\theta)}{2} + \frac{h_t - h_b}{4R}\frac{\partial w(x,\theta)}{\partial \theta} \\ &+ \frac{2z}{h_c}\left(\frac{v_1(x,\theta)-v_2(x,\theta)}{2} + \frac{h_t + h_b}{4R}\frac{\partial w(x,\theta)}{\partial \theta}\right) \end{aligned} \quad (3b)$$

$$w_c(x,\theta,z) = w(x,\theta) \quad (3c)$$

According to the classical Love's shell theory, the strain components in the upper and lower faces of the considered shell are as follows (Soedel 2004)

$$\varepsilon_x^i = \frac{\partial u_i(x,\theta,z)}{\partial x} \qquad ; i = t, b \quad (4a)$$

$$\varepsilon_\theta^i = \frac{1}{R_i}\frac{\partial v_i(x,\theta,z)}{\partial \theta} - \frac{w(x,\theta)}{R_i} \qquad ; i = t, b \quad (4b)$$

$$\gamma_{x\theta}^i = \frac{\partial v_i(x,\theta,z)}{\partial x} + \frac{1}{R_i}\frac{\partial u_i(x,\theta,z)}{\partial \theta} \qquad ; i = t, b \quad (4c)$$

where the subscripts x and θ address the longitudinal and circumferential directions, respectively. Also, the out of plane shear components of strain field in the core are as follows

$$\gamma_{xz}^c = \frac{\partial w(x,\theta)}{\partial x} + \frac{\partial u_c(x,\theta,z)}{\partial z} \quad (5a)$$

$$\gamma_{\theta z}^c = \frac{\partial v_c(x,\theta,z)}{\partial z} + \frac{1}{R-z}\frac{\partial w(x,\theta)}{\partial \theta} + \frac{v_c(x,\theta,z)}{R-z} \quad (5b)$$

3.2 Stress-strain relations

Both faces and core isotropic materials will undergo an elastic deformation. From infinitesimal point of view the general form for the in-plane stresses vs. strains relations in elastic range for both faces will be (Soedel 2004)

$$\sigma_x^i = \frac{E^i}{1-\nu_i^2}\left(\varepsilon_x^i + \nu_i \varepsilon_\theta^i\right) = C_{11}^i \varepsilon_x^i + C_{12}^i \varepsilon_\theta^i \quad ; i = t, b \quad (6a)$$

$$\sigma_\theta^i = \frac{E^i}{1-\nu_i^2}\left(\varepsilon_\theta^i + \nu_i \varepsilon_x^i\right) = C_{12}^i \varepsilon_x^i + C_{22}^i \varepsilon_\theta^i \quad ; i = t, b \quad (6b)$$

$$\tau_{x\theta}^i = \frac{E^i}{2(1+\nu_i)}\gamma_{x\theta}^i = C_{33}^i \gamma_{x\theta}^i \quad ; i = t, b \quad (6c)$$

where E and v are the Young's modulus and Poisson's ratio, respectively.

Based on aforementioned assumptions, the general form for shear stresses vs. shear strains relations in elastic range of the core section made of an isotropic material will be

$$\tau_{iz}^c = G_c \gamma_{iz}^c \qquad ; i = x, \theta \quad (7)$$

where G_c is the elastic shear modulus of the core.

4. Governing equations and solution procedure

In order to arrive to the governing differential equations in the considered shell geometry, the principle of the stationary potential energy is employed (Washizu 1975)

$$\delta\Pi = \delta(U - W) = 0 \quad (8)$$

where Π, U and W are the total potential energy, deformation energy and the work done by the external loadings, respectively.

The total deformation energy can be expressed as the summation of deformation energy of each part that is, top, bottom faces and the core section as

$$U = U_t + U_c + U_b \quad (9)$$

Moreover, the total deformation energy can be also expressed in terms of stress and strain components as (Washizu 1975)

$$\begin{aligned} U &= \frac{1}{2}\int_{V_t} (\sigma_x^t \varepsilon_x^t + \sigma_\theta^t \varepsilon_\theta^t + \tau_{x\theta}^t \gamma_{x\theta}^t) dV_t \\ &+ \frac{1}{2}\int_{V_c} (\tau_{xz}^c \gamma_{xz}^c + \tau_{\theta z}^c \gamma_{\theta z}^c) dV_c \\ &+ \frac{1}{2}\int_{V_b} \left(\sigma_x^b \varepsilon_x^b + \sigma_\theta^b \varepsilon_\theta^b + \tau_{x\theta}^b \gamma_{x\theta}^b\right) dV_b \end{aligned} \quad (10)$$

in which subscript t, c and b are addressing the top, core and bottom parts of the shell. After substituting stress relations from Eqs. (6) and (7) in Eq. (10), one would get

$$\begin{aligned} U &= \frac{R_t}{2}\int_{-h_c/2-h_t}^{-h_c/2}\int_0^\beta\int_0^L (C_{11}^t(\varepsilon_x^t)^2 + 2C_{12}^t \varepsilon_x^t \varepsilon_\theta^t \\ &\qquad + C_{22}^t(\varepsilon_\theta^t)^2 + C_{33}^t(\gamma_{x\theta}^t)^2)\, dx\, d\theta\, dz \\ &+ \frac{R}{2}\int_{-h_c/2}^{h_c/2}\int_0^\beta\int_0^L (G_c(\gamma_{xz}^t)^2 + G_c(\gamma_{\theta z}^t)^2)\, dx\, d\theta\, dz \\ &+ \frac{R_b}{2}\int_{h_c/2}^{h_c/2+h_b}\int_0^\beta\int_0^L \left(C_{11}^b(\varepsilon_x^b)^2 + 2C_{12}^b \varepsilon_x^b \varepsilon_\theta^b \right. \\ &\qquad \left. + C_{22}^b\left(\varepsilon_\theta^b\right)^2 + C_{33}^b\left(\gamma_{x\theta}^b\right)^2\right) dx\, d\theta\, dz \end{aligned} \quad (11)$$

Now, by substituting strains in terms of displacement field in Eq. (11), U becomes a function of displacement. For brevity, this expression has not been given here.

Also the work done due to external loads in terms of displacement filed is

$$W = \int_0^{\beta}\int_0^{L} q_t(x,\theta)\, w(x,\theta)\, R_t\, dx\, d\theta + \int_0^{\beta}\int_0^{L} q_b(x,\theta)\, w(x,\theta)\, R_b\, dx\, d\theta \tag{12}$$

in which $q(x,\theta)$ represents the shape of distributive external loading. Having on hand the U and W in terms of displacement components, one can establish the expression for the total potential energy. After substituting displacement field in the total potential energy expression then one can impose the minimization principle.

By doing this, the governing coupled differential equations and related boundary conditions are obtained in terms of displacement components, which are presented in Appendix A.

For solving the obtained equations, the HDQM is used. In this method, the partial derivative of a function, with respect to a spatial variable at a given discrete point, approximated by a linear summation of weighted function values at all discrete points chosen in the solution domain of the spatial variable. Suppose the domain of considered shell are represented by ($0 < x < L$, $0 < \theta < \beta$) and being discretized by $N_x \times N_\theta$ grid points along x and θ coordinates. If $F(x, \theta)$ representing either of deformation functions; *(u, v, w)* within the shell domain, then the partial derivatives of $F(x, \theta)$ with respect to x and θ at the point (x_i, θ_j) can be expressed discretely as (Civalek 2004)

$$\frac{d^n F(x_i,\theta_j)}{dx^n} = \sum_{k=1}^{N_x} A_{ik}^{(n)} F(x_k,\theta_j)\,;\; n = 1,2,\ldots,N_x - 1; \tag{13}$$

$$\frac{d^m F(x_i,\theta_j)}{d\theta^m} = \sum_{l=1}^{N_\theta} B_{jl}^{(m)} F(x_i,\theta_l)\,;\; m = 1,2,\ldots,N_\theta - 1; \tag{14}$$

$$\frac{d^{n+m} F(x_i,\theta_j)}{dx^n\, d\theta^m} = \sum_{k=1}^{N_x}\sum_{l=1}^{N_\theta} A_{ik}^{(n)} B_{jl}^{(m)} F(x_k,\theta_l)\,; \quad n = 1,2,\ldots,N_x - 1;\; m = 1,2,\ldots,N_\theta - 1; \tag{15}$$

where $A_{ik}^{(n)}$ and $B_{jl}^{(m)}$ are the weighting coefficients in conjunction to the order of partial derivative of $F(x, \theta)$ with respect to x, i.e., n and the order of derivative with respect to θ, i.e., m at the discrete points x_i and θ_j, respectively. The description of HDQ method and how to choose the positions of the grid points using Chebyshev polynomials can be found in detail in (Civalek 2004). Now, the HDQM can be used to discretize the coupled Eqs. (A1)-(A5), governing equations, (A6)-(A11), boundary condition equations for straight edges, and (A12)-(A17), boundary condition equations for curved edges. The discretized forms of all 17 equations using HDQM are obtained. However, in order to avoid repetitive representations on this regard, only the discretized form of Eq. (A1) is presented in this study, as shown in the Appendix B.

For any sort of boundary conditions, after separating domain and boundary degrees of freedom (DOF), the following assembled matrix equations are obtained

$$\begin{bmatrix} [K_{bb}] & [K_{bd}] \\ [K_{db}] & [K_{dd}] \end{bmatrix} \begin{Bmatrix} \{d^b\} \\ \{d^d\} \end{Bmatrix} = \begin{Bmatrix} 0 \\ \{P\} \end{Bmatrix} \tag{16}$$

where $\{d^b\}$ and $\{d^d\}$ represent the boundary and domain DOF, respectively, and $\{P\}$ is the load vector. After doing some mathematical simplifications on Eq. (16), the displacement components can be calculated by solving the following relation

$$\left[[K_{dd}] - [K_{db}][K_{bb}]^{-1}[K_{bd}]\right]\{d^d\} = \{P\} \tag{17}$$

Based on the above outlined formulations, and by aids of the MATLAB program solver a self-developed computer program is written by which the displacements, strains and stresses in different points of the shell faces and core can be obtained. Again it should be emphasized that no limitations on the type of boundary conditions and loading exist on solving these equations.

4. Results and discussions

Primarily, to check on the convergences of the results as the initial step in employing the HDQ method, several cases with different number of grid points were examined. Also, two types of grid points including equally and non-equally spaced, are used. In the case of the non-equally spaced grid points the positions of the grid points are determined using Chebyshev polynomials. More details about this issue can be found in (Striz *et al.* 1995, Civalek and Ülker 2004). Briefly, the outcome of this part indicated that the selection a non-equally spaced grid with minimum 21×21 points will yield to a stable answer in the problem under consideration. Therefore, in all up-coming case studies in this section, this gird scheme has been used. For example, for a cylindrical sandwich shell panel with clamped edges subjected to a uniform lateral loading of q_t = 1 kPa the convergence of the solution for the central transverse displacement w of the shell panel, is presented in Fig. 2. The geometrical parameters are L = 0.9 m, R = 1.2 m, β = 35°, h_t = 1 mm, h_b = 1 mm, h_c = 10 mm (Fig. 1). Also, the structural steel with E_f = 210 GPa, ν_f = 0.3, has been chosen for both face materials. The core material is AirexR63.50 (Rao 2002) with E_c= 37.5 MPa and G_c = 14.05 MPa.

In order to show the independency of the solution method to the loading type, in addition to the uniform lateral loading, which is generally used in static analysis, the sinusoidal loading is also applied. The obtained results using HDQM are compared with those similar ones acquired from FEM.

5.1 Case study 1: Evaluation of proper functionality and verification

A cylindrical sandwich shell subjected to uniform lateral pressure is considered. The geometrical parameters are L =

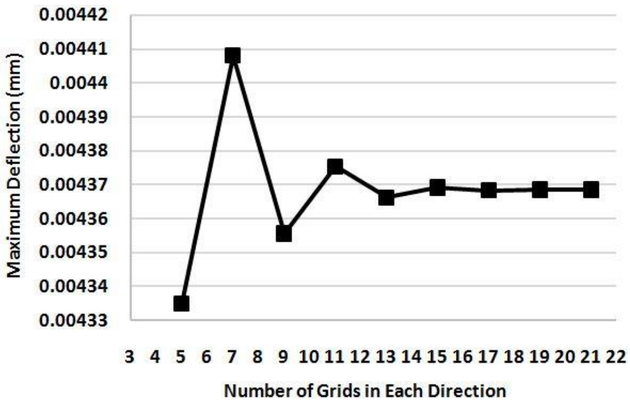

Fig. 2 The maximum lateral deflection of the shell panel with clamped edges, for different grid points

free (F) are considered (for example, *CFSS* denotes a cylindrical shell with clamped one curved edge, free one axial edge and simply supported two other edges). Note that the details of boundary conditions are presented in the end of Appendix A.

The comparison of the results in Table 1 shows a very good agreement between the HDQM and FEM results.

It has to be mentioned that in constructing the FE model, the ANSYS software (version 13) has been used. The FE model comprises 11892 three dimensional 20-node brick type elements with total number of nodes of 85273. The faces and the core are modeled as linear elastic materials. The static analyses are done in the software. It is to be noted that the core and the faces are modeled as 3D solids, so that no restricting assumptions such as neglecting the in-plane stresses in the core or neglecting the out-of-plane stresses in the x are imposed in finite element modeling.

Table 1 Maximum deflection of the shell, for lateral pressure of q_t = 100 Pa

B.C.s	**FEM** (10^{-6} m)	**HDQM** (10^{-6} m)	**%disc.***	**B.C.s**	**FEM** (10^{-6} m)	**HDQM** (10^{-6} m)	**%disc.**
CCCC	0.4387	0.4369	0.39	SSSS	3.3060	3.2320	2.26
CSCC	3.0450	2.9890	1.86	SSCS	3.0680	3.0070	2.00
CCSC	0.4163	0.4151	0.29	SCSC	0.4069	0.4048	0.50
CSCS	2.8263	2.7822	1.56	SCSS	3.8295	3.7223	2.80
CCSS	3.4090	3.3170	2.70	CFCF	15.614	15.177	2.80
CFCC	18.177	17.8135	2.00	CFSS	21.971	21.629	1.55

*%disc. = (FEM-HDQM)/FEM×100

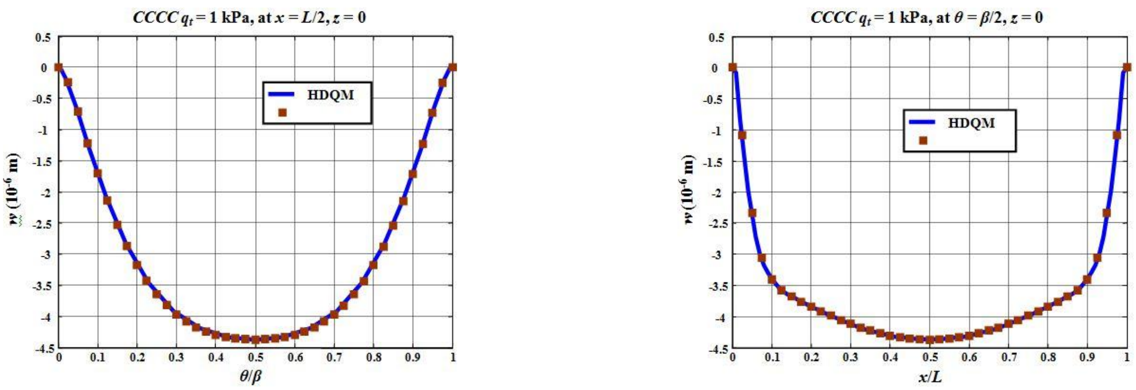

(a) (b)

Fig. 3 Transverse deflection in core mid-surface for uniform loading along θ (a) and x (b) directions

0.9 m, R = 1.2 m, β = 35°, h_t = 1 mm, h_b = 1 mm, h_c = 10 mm (see Fig. 1). Also, the structural steel with E_f = 210 GPa, ν_f = 0.3, has been chosen for both face materials. The core material is AirexR63.50 (Rao 2002) with E_c= 37.5 MPa and G_c = 14.05 MPa.

Based on the above data the developed program was executed out of which for the sandwich shell with different boundary conditions, the values of maximum shell deflection are obtained. The results related to the maximum lateral deflection of the shell under lateral uniform pressure of q_t = 100 Pa are compared with those obtained using FEM in Table 1. In this table various combinations of boundary conditions including simply supported (S), clamped (C) and

The variations of the transverse deflection w in the core mid-surface along θ and x directions are presented in Fig. 3, for the shell with all edges clamped and under uniform pressure of q_t = 1 kPa. For this shell, distributions of transverse shear stresses, τ_{xz} and $\tau_{\theta z}$, of core mid-surface along x direction are shown in Fig. 4. In addition, in-plane normal stress $\sigma_{\theta\theta}$ of top and bottom surfaces of shell along θ direction and in-plane normal stress σ_{xx} of top and bottom surfaces of shell along x direction are shown in Fig. 5 and 6, respectively. In all above cases, the FEM results are also shown along with the HDQM results. A close inspection of

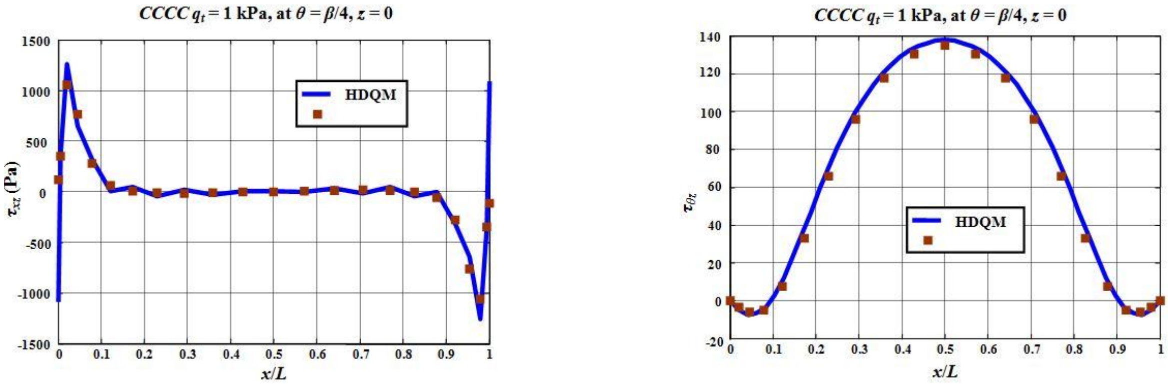

(a) (b)

Fig. 4 Transverse shear stresses, τ_{xz} (a) and $\tau_{\theta z}$ (b), in core mid-surface along x direction for uniform loading

these results indicates very good agreement between the HDQM and FEM results. Note that based on the Saint-Venant's principle the results near to the boundaries cannot be trusted.

It should be further clarified that for a case of cylindrical sandwich shell under *CCCC* type of boundary conditions, the CPU time used in solving this problem by the self-developed program based on implementation of HDQM and a FEM model comprising 11892 of 20-noded brick type elements with total number of nodes of 85273 reveals a minimum 50.6% saving in CPU time with respect to the FEM model. Furthermore, it has been verified that upon equal number of nodes in a specified grid size, the developed program based of HDQ method leads to a more accurate result than FEM. Note that this advantage of the DQ methods over FEM has been frequently reported by other researchers as well (Civalek 2004, Maleki *et al.* 2012, Bozdogan 2012).

Similar analysis was performed for a sandwich shell with the same geometrical and material parameters

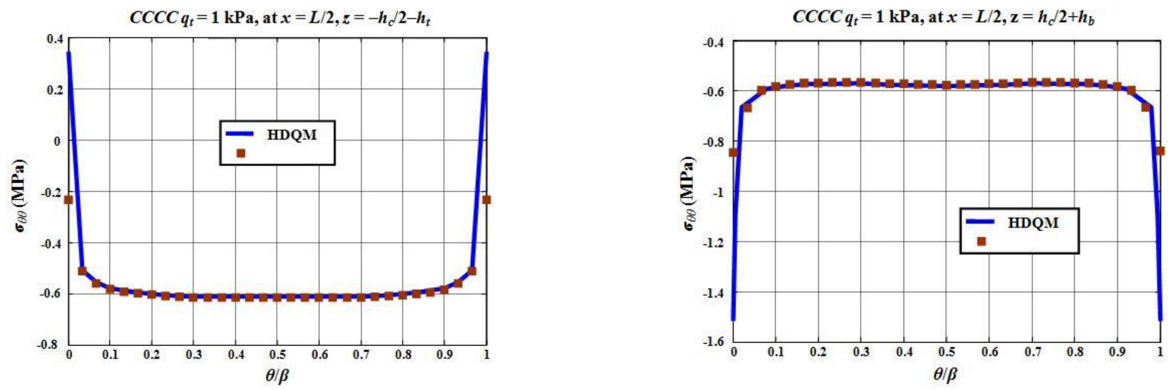

(a) (b)

Fig. 5 In-plane normal stress $\sigma_{\theta\theta}$ of top (a) and bottom (b) surfaces of shell along θ direction for uniform loading

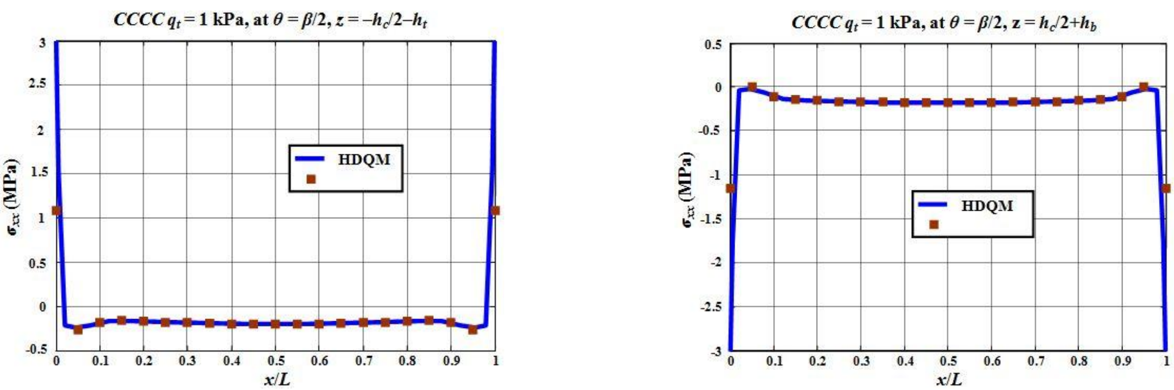

(a) (b)

Fig. 6 In-plane normal stress σ_{xx} of top (a) and bottom (b) surfaces of shell along x direction for uniform loading

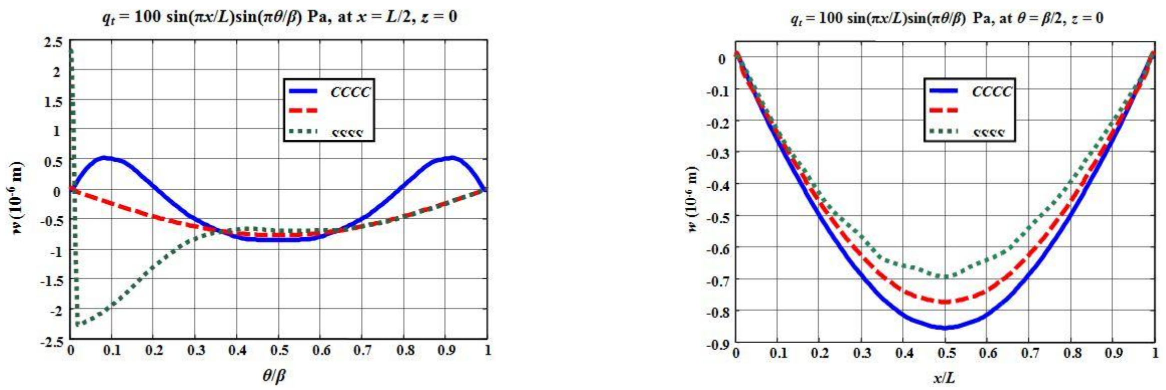

(a) (b)

Fig. 7 Transverse deflection in core mid-surface for sinusoidal loading along θ (a) and x (b) directions

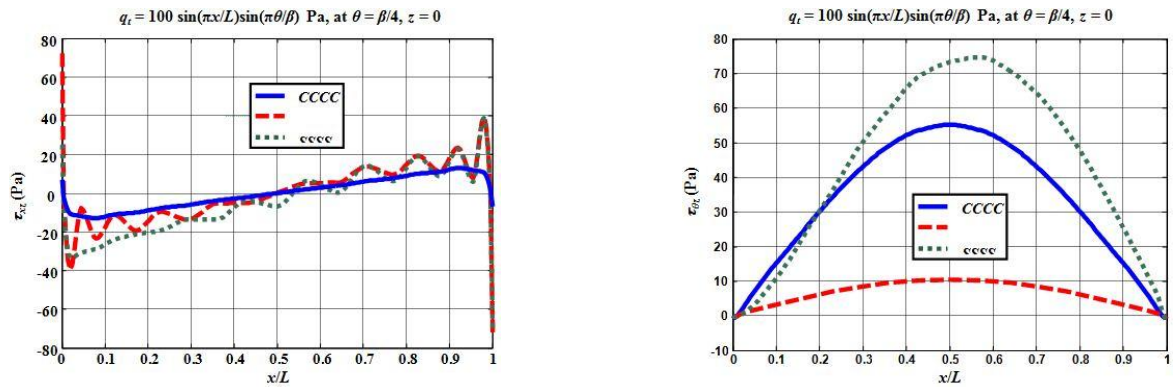

(a) (b)

Fig. 8 Transverse shear stresses, τ_{xz} (a) and $\tau_{\theta z}$ (b), in core mid-surface along x direction for sinusoidal loading

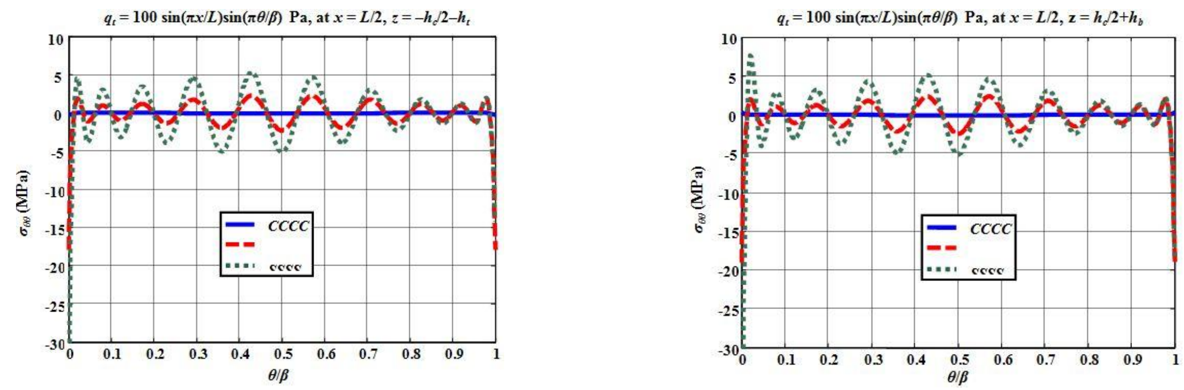

(a) (b)

Fig. 9 In-plane normal stress $\sigma_{\theta\theta}$ of top (a) and bottom (b) surfaces of shell along θ direction for sinusoidal loading

subjected to sinusoidal lateral pressure. For the loading function a loading of the form $q_t(x,\theta) = q_0 \sin\left(\frac{\pi x}{L}\right) \sin\left(\frac{\pi\theta}{\beta}\right)$ is considered. By setting the q_0 = 100 Pa and under three different boundary conditions namely; *CCCC*, *SSSS* and *CFSS*, the variations of transverse deflection w in core mid-surface along θ and x directions are depicted in Fig. 7. For this shell, distributions of transverse shear stresses, τ_{xz} and $\tau_{\theta z}$, of core mid-surface along x direction are shown in Fig. 8. In addition, in-plane normal stress $\sigma_{\theta\theta}$ of top and bottom surfaces of shell along θ direction and in-plane normal stress σ_{xx} of top and bottom surfaces of shell along x direction are shown in Figs. 9 and 10, respectively. Note that in this case only the results of HDQM are presented.

5.2 Case study 2: Effects of core flexibility

To investigate on the effect of core flexibility, another study is performed. In this case all edges of sandwich shell under uniform pressure of q_t = 1 kPa are clamped.

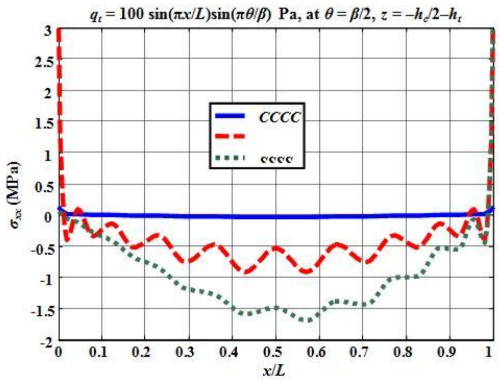

(a)

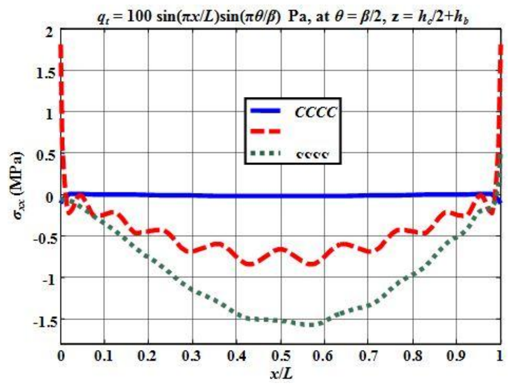

(b)

Fig. 10 In-plane normal stress σ_{xx} of top (a) and bottom (b) surfaces of shell along x direction for sinusoidal loading

Table 2 Transverse displacement, w (10^{-6}m) at $x = L/3$, $\theta = \beta/3$ and $z = 0$

E_f/E_c	$h_c/h_f = 5$			$h_c/h_f = 10$			$h_c/h_f = 20$		
	HDQM	FEM	%disc.	HDQM	FEM	%disc.	HDQM	FEM	%disc.
210	-4.0165	-3.9797	*0.92*	-4.0561	-3.9882	*1.70*	-3.7505	-3.6287	*3.36*
525	-3.8628	-3.8474	*0.40*	3.9330	-3.9118	*0.54*	-3.8051	-3.7679	*0.99*
1050	-3.7148	-3.7011	*0.37*	-3.8034	-3.7921	*0.30*	-3.7949	-3.7828	*0.32*
2625	-3.5052	-3.4856	*0.56*	-3.6101	-3.5991	*0.31*	-3.6939	-3.6917	*0.06*
5250	-3.3493	-3.3225	*0.81*	-3.4613	3.4460	*0.44*	3.5740	-3.5706	*0.10*
10500	-3.2029	-3.1682	*1.10*	-3.3131	-3.2908	*0.68*	-3.4372	3.4290	*0.24*

Table 3 In-plane normal stress, σ_{xx} (Pa) at $x = L/3$, $\theta = \beta/3$ and $z = -h_c/2-h_t$

E_f/E_c	$h_c/h_f = 5$			$h_c/h_f = 10$			$h_c/h_f = 20$		
	HDQM	FEM	%disc.	HDQM	FEM	%disc.	HDQM	FEM	%disc.
210	-193130	-187470	*3.02*	-222210	-214460	*3.61*	-246700	-234740	*5.09*
525	-188100	-186320	*0.96*	-204000	-201500	*1.24*	-216260	-212850	*1.60*
1050	-183570	-183470	*0.05*	-191200	-190920	*0.15*	-196090	-196010	*0.04*
2625	-177800	-178460	*-0.37*	-179980	-181120	*-0.63*	-180230	-182620	*-1.31*
5250	-174070	-174930	*-0.49*	-175270	-177030	*-0.99*	-175030	-178910	*-2.17*
10500	-171000	-172380	*-0.80*	-172090	-174960	*-1.64*	-172350	-178640	*-3.52*

Furthermore, the geometry of the shell comprises of the following parameters; L = 0.9 m, R = 1.2 m, β = 60°, h_t = 1 mm, h_b = 1 mm, h_c = 10 mm. The faces are made of the structural steel with mechanical properties of the same as the one considered in Section 5.1. Nonetheless, several isotropic materials are selected for the core material with the values of their E_c, varying in the range of 20 to 1000 MPa. This problem was solved thoroughly and out of different obtained results only the variation of transverse displacement at core mid-surface, in-plane normal stress σ_{xx} on the external surface of shell and in-plane normal stress $\sigma_{\theta\theta}$ on the internal surface of shell are listed in Tables 2, 3 and 4, respectively, for six different ratios of E_f/E_c and three different ratios of h_c/h_f. As indicated in these tables, comparison of these results shows very good agreement between HDQM and suitably developed FEM model (at the worst case about 3.52% error in the case of σ_{xx}). Moreover, no specific trend can be seen in increasing or decreasing the core flexibility of the shell by changing E_f/E_c ratios.

5.3 Case study 3: Effects of geometric parameters

Referred to different indicated geometrical parameters, two important ratios are studied in this section. The first one is the core to the face thickness ratio (h_c/h_f) and the second one is the ratio of shell curvature to thickness (R/h).

To study the core to the face thickness ratio a cylindrical sandwich shell with clamped edges (CCCC) subjected to uniform lateral pressure of q_t = 1 kPa is considered. The geometrical parameters are L = 0.9 m, R = 1.2 m, β = 60°, h_t = 1 mm, h_b = 1 mm and h_c has some values between 5 and 40 mm. Also, the faces and the core materials are made of the structural steel and AirexR63.50, respectively, whose properties are given in Section 5.1.

Table 4 In-plane normal stress, $\sigma_{\theta\theta}$ (Pa) at $x = L/3$, $\theta = \beta/3$ and $z = h_c/2+h_b$

E_f/E_c	$h_c/h_f = 5$			$h_c/h_f = 10$			$h_c/h_f = 20$		
	HDQM	**FEM**	**%disc.**	**HDQM**	**FEM**	**%disc.**	**HDQM**	**FEM**	**%disc.**
210	-584800	-584910	*-0.02*	-546680	-543050	*0.67*	-464480	-457300	*1.57*
525	-586240	-589700	*-0.59*	-562860	-565510	*-0.47*	-515920	-519390	*-0.67*
1050	-589900	-593780	*-0.65*	-576170	-579960	*-0.65*	-551940	-558580	*-1.19*
2625	-597220	-599870	*-0.44*	-591260	-593820	*-0.43*	-583640	-589980	*-1.07*
5250	-602310	-602960	*-0.11*	-599320	-598960	*0.06*	-596430	-598650	*-0.38*
10500	-605740	-603290	*0.41*	-604480	-598760	*0.96*	-603640	-596530	*1.19*

Table 5 Transverse displacement and in-plane normal stresses at $x = L/3$ and $\theta = \beta/3$

h_c/h_f	w (10^{-6} m) at $z = 0$			σ_{xx} (Pa) at $z = -h_c/2-h_t$			$\sigma_{\theta\theta}$ (Pa) at $z = h_c/2+h_b$		
	HDQM	**FEM**	**%disc.**	h_c/h_f	**HDQM**	**FEM**	**HDQM**	**FEM**	**%disc.**
5	-3.3493	-3.3225	*0.81*	-174070	-174930	*-0.49*	-602310	-602960	*-0.11*
10	-3.4613	3.4460	*0.44*	-175270	-177030	*-0.99*	-599320	-598960	*0.06*
20	3.5740	-3.5706	*0.10*	-175030	-178910	*-2.17*	-596430	-598650	*-0.38*
40	-3.6639	-3.6667	*-0.08*	-172280	-177140	*-2.74*	-593250	-584030	*1.58*

Table 6 Transverse displacement and in-plane normal stresses at $x = L/3$ and $\theta = \beta/$

	R/h	w (10^{-6} m) at $z = 0$			σ_{xx} (Pa) at $z = -h_c/2-h_t$			$\sigma_{\theta\theta}$ (Pa) at $z = h_c/2+h_b$		
		HDQM	**FEM**	**%disc.**	**HDQM**	**FEM**	**%disc.**	**HDQM**	**FEM**	**%disc.**
h = 12 mm	500	-64.222	-63.034	*1.88*	-376410	-394710	*-4.64*	-2654000	-2655800	*-0.07*
	100	-2.9524	-2.9446	*0.26*	-156030	-155000	*0.66*	-551250	-555130	*-0.70*
	50	-0.8403	-0.8499	*-1.13*	-81551	-80463	*1.35*	-276140	-285660	*-3.33*
	20	-0.1486	-0.1523	*-2.44*	-31592	-27781	*13.72*	-110850	-131610	*-15.77*
R = 1.2 m	200	-6.7320	-6.8166	*-1.24*	-355710	-339370	*4.81*	-1207300	-1209300	*-0.17*
	100	-3.4264	-3.4495	*0.67*	-170990	-166570	*2.65*	-602660	-609740	*1.16*
	50	-1.7594	-1.7686	*0.52*	-83606	-80148	*4.31*	-299460	-315500	*5.08*
	25	-0.92587	-0.94033	*-1.54*	-41372	-34717	*19.2*	-149080	-176470	*15.5*

The obtained values of transverse displacement at core mid-surface, in-plane normal stress σ_{xx} of top surface of shell and in-plane normal stress $\sigma_{\theta\theta}$ of bottom surface of shell for four different thickness ratios at specified places are listed in Table 5. All results show very good agreement between HDQM and FEM. As indicated in this table, comparison of these results shows very good agreement (at the worst case about 2.74% error in the case of σ_{xx}) between HDQM and suitably developed FEM model.

To study the variation effect of the curvature to thickness ratio, a cylindrical sandwich shell with clamped edges (CCCC) subjected to a uniform lateral pressure of q = 1 kPa is considered. The geometrical parameters are L = 0.9 m, β = 60°, $h_t = h_b = h_c/10$ and the problem has been solved for four different values of R/h from 20 to 500. Also, the faces and the core materials are made of structural steel and AirexR63.50, respectively, with mechanical properties the same as those used in the case study 1.

The obtained values of transverse displacement at core mid-surface, in-plane normal stress σ_{xx} on the external surface of shell and in-plane normal stress $\sigma_{\theta\theta}$ on the internal surface of shell are listed in Table 6. This table shows that by decreasing the curvature to thickness ratio, the difference between HDQM and FEM increases. The comparison of the results indicate that for the ratios of 20 or less, implementation of the classical theory will yield to unsatisfactory results and hence, using another shell theory may resolve this shortcomings.

5. Conclusions

Cylindrical sandwich shells under general type of distributive lateral loadings are modeled based on a classical theory of sandwich structures. The faces are modeled as thin cylindrical shells obeying the Kirchhoff-Love assumptions. For the core material it is assumed to be thick and the in-plane stresses are negligible. The governing equations are derived using the principle of the stationary potential energy and solved using harmonic differential quadrature method (HDQM). The obtained results using HDQM are compared by results out of the finite element method solutions. Based on this study, following are concluded:

- In using HDQM for static analysis of sandwich shells, there are no limits on type of boundary conditions and loadings.
- The HDQM leads to more accurate results than FEM for the same number of grid points.
- By increasing the core to the face thickness ratio and the curvature to thickness ratio, the transverse displacement at core mid-surface increases.

By decreasing the curvature to thickness ratio, the difference between the obtained results using classical theory and FEM increases. The results show that for the R/h ratios of less than 20, the obtained results using classical theory are not trustable, especially for stresses.

References

Abouhamze, M., Aghdam, M.M. and Alijani, F. (2007), "Bending analysis of symmetrically laminated cylindrical panels using the extended Kantorovich method", *Mech. Adv. Mater. Struct.*, **14**(7), 523-530.

Alankaya, V. and Oktem, A.S. (2016), "Static analysis of laminated and sandwich composite doubly-curved shallow shells", *Steel Compos. Struct., Int. J.*, **20**(5), 1043-1066.

Allahkarami, F., Nikkhah-Bahrami, M. and Saryazdi, M.G. (2017), "Damping and vibration analysis of viscoelastic curved microbeam reinforced with FG-CNTs resting on viscoelastic medium using strain gradient theory and dqm", *Steel Compos. Struct., Int. J.*, **25**(2), 141-155.

Allen, H.G. (1969), *Analysis and Design of Structural Sandwich Panels*, Pergamon Press Inc., Oxford, UK.

Altenbach, H. (2011), "Mechanics of advanced materials for lightweight structures", *Proceedings of the Institution of Mechanical Engineers, Part C: Journal of Mechanical Engineering Science*, **225**(11), 2481-2496.

Altenbach, H., Altenbach, J. and Kissing, W. (2004), *Mechanics of Composite Structural Elements*, Springer, New York, USA.

Baltacıoglu, A.K., Akgoz, B. and Civalek, Ö. (2010), "Nonlinear static response of laminated composite plates by discrete singular convolution method", *Compos. Struct.*, **93**(1), 153-161.

Bellman, R., Kashef, B.G. and Casti, J. (1972), "Differential quadrature: A technique for the rapid solution of nonlinear partial differential equations", *J. Comput. Phys.*, **10**(1), 4-52.

Bhimaraddi, A. and Chandrashekhara, K. (1992), "Three-dimensional elasticity solution for static response of simply supported orthotropic cylindrical shells", *Compos. Struct.*, **20**(4), 227-235.

Bozdogan, K.B. (2012), "Differential quadrature method for free vibration analysis of coupled shear walls", *Struct. Eng. Mech., Int. J.*, **41**(1), 67-81.

Carrera, E. (2003), "Historical review of Zig-Zag theories for multilayered plates and shells", *Appl. Mech. Rev.*, **56**(3), 287-308.

Carrera, E. (2004), "On the use of the Murakami's zig-zag function in the modeling of layered plates and shells", *Comput. Struct.*, **82**(7-8), 541-554.

Civalek, Ö. (2004), "Application of differential quadrature (DQ) and harmonic differential quadrature (HDQ) for buckling analysis of thin isotropic plates and elastic columns", *Eng. Struct.*, **26**(2), 171-186.

Civalek, Ö. (2007a), "Linear vibration analysis of isotropic conical shells by discrete singular convolution (DSC)", *Struct. Eng. Mech., Int. J.*, **25**(1), 127-130.

Civalek Ö. (2007b), "A parametric study of the free vibration analysis of rotating laminated cylindrical shells using the method of discrete singular convolution", *Thin-Wall. Struct.*, **45**(7-8), 692-698.

Civalek, Ö. (2008a), "Vibration analysis of conical panels using the method of discrete singular convolution", *Commun. Numer. Meth. Eng.*, **24**(3), 169-181.

Civalek, Ö. (2008b), "Analysis of thick rectangular plates with symmetric cross-ply laminates based on first-order shear deformation theory", *J. Compos. Mater.*, **42**(26), 2853-2867.

Civalek, Ö. and Gürses, M. (2009), "Free vibration analysis of rotating cylindrical shells using discrete singular convolution technique", *Int. J. Pres. Ves. Pip.*, **86**(10), 677-683.

Civalek, Ö. and Ülker, M. (2004), "Harmonic differential quadrature (HDQ) for axisymmetric bending analysis of thin isotropic circular plates", *Struct. Eng. Mech., Int. J.*, **17**(1), 1-14.

Gürses, M., Civalek, Ö., Korkmaz, A. and Ersoy, H. (2009), "Free vibration analysis of symmetric laminated skew plates by discrete singular convolution technique based on first-order shear deformation theory", *Int. J. Numer. Meth. Eng.*, **79**(3), 290-313.

Gürses, M., Akgöz, B. and Civalek, Ö. (2012), "Mathematical modeling of vibration problem of nano-sized annular sector plates using the nonlocal continuum theory via eight-node discrete singular convolution transformation", *Appl. Math. Comput.*, **219**(6), 3226-3240.

Hamzehkolaei, N.S., Malekzadeh, P. and Vaseghi, J. (2011), "Thermal effect on axisymmetric bending of functionally graded circular and annular plates using dqm", *Steel Compos. Struct., Int. J.*, **11**(4), 341-358.

Jaskula, L. and Zielnica, J. (2011), "Large displacement stability analysis of elastic-plastic unsymmetrical sandwich cylindrical shells", *Thin Wall. Struct.*, **49**(5), 611-617.

Librescu, L. and Hause, T. (2000), "Recent developments in the modeling and behavior of advanced sandwich constructions: a survey", *Compos. Struct.*, **48**(1-3), 1-17.

Maleki, S., Tahani, M. and Andakhshideh, A. (2012), "Static and transient analysis of laminated cylindrical shell panels with various boundary conditions and general lay-ups", *ZAMM Z. Angew. Math. Mech.*, **92**(2), 124-140.

Malekzadeh, P. (2009), "A two-dimensional layerwise-differential quadrature static analysis of thick laminated composite circular arches", *Appl. Math. Model.*, **33**(4), 1850-1861.

Mohammadimehr, M. and Shahedi, S. (2016), "Nonlinear magneto-electro-mechanical vibration analysis of double-bonded sandwich Timoshenko microbeams based on MSGT using Gdqm", *Steel Compos. Struct., Int. J.*, **21**(1), 1-36.

Ng, T.Y. and Lam, K.Y. (1999), "Effects of elastic foundation on the dynamic stability of cylindrical shells", *Struct. Eng. Mech., Int. J.*, **8**(2), 193-205.

Noor, A.K., Burton, W.S. and Bert, C.W. (1996), "Computational models for sandwich panels and shells", *Appl. Mech. Rev.*, **49**(3), 155-199.

Plantema, F.J. (1966), *Sandwich Construction*, John Wiley & Sons, New York, USA.

Rao, T. (2002), "Study of core compression using digital image correlation (DIC)", Master of Science Dissertation; Michigan Technological University.

Shu, C. (2000), *Differential Quadrature and its Application in Engineering*, Springer, Berlin, Germany.

Shu, C. and Richards, B.E. (1992), "Application of generalized differential quadrature to solve two-dimensional incompressible

Navier Stockes equations", *Int. J. Numer. Meth. Fl.*, **15**(7), 791-798.
Soedel, W. (2004), *Vibrations of Shells and Plates*, Marcel Dekker Inc., New York, USA.
Striz, A.G., Wang, X. and Bert, C.W. (1995), "Harmonic differential quadrature method and applications to analysis of structural components", *Act. Mech.*, **111**(1-2), 85-94.
Tornabene, F., Liverani, A. and Caligiana, G. (2012), "Static analysis of laminated composite curved shells and panels of revolution with aposteriori shear and normal stress recovery using generalized differential quadrature method", *Int. J. Mech. Sci.*, **61**(1), 71-87.
Tornabene, F., Fantuzzi, N., Ubertini, F. and Viola, E. (2015), "Strong formulation finite element method based on differential quadrature: A survey", *Appl. Mech. Rev.*, **67**(2), 020801-020801-55.
Tornabene, F., Fantuzzi, N. and Bacciocchi, M. (2017), "Foam core composite sandwich plates and shells with variable stiffness: Effect of the curvilinear fiber path on the modal response", *J. Sandw. Struct. Mater.* DOI: 10.1177/1099636217693623
Vinson, J.R. (2001), "Sandwich structures", *Appl. Mech. Rev.*, **54**(3), 201-214.
Washizu, K. (1975), *Variational Methods in Elasticity and Plasticity*, Pergamon Press, Oxford, UK.
Zhong, H. and Yu, T. (2009), "A weak form quadrature element method for plane elasticity problems", *Appl. Math. Model.*, **33**(10), 3801-3814.
Zhao, X., Ng, T.Y. and Liew, K.M. (2004), "Free vibration of two-side simply supported laminated panels via the mesh-free Kp-Ritz method", *Int. J. Mech. Sci.*, **46**(1), 123-142.
Zenkert, D. (1995), *An Introduction to Sandwich Construction*, Chameleon Press, London, UK.

CC

Appendix A

Governing Equations

$$-\frac{G_cR}{h_c}u_2+\frac{G_cR}{h_c}u_1-\frac{C_{23}^t h_t}{R_t}\frac{\partial w}{\partial\theta}-\frac{C_{33}^t h_t}{R_t}\frac{\partial^2 u_1}{\partial\theta^2}-\frac{C_{23}^t h_t}{R_t}\frac{\partial^2 v_1}{\partial\theta^2}+\left(-C_{12}^t h_t+G_{xz}R\frac{h_b+2h_c+h_t}{2h_c}\right)\frac{\partial w}{\partial x}$$
$$-2C_{13}^t h_t\frac{\partial^2 u_1}{\partial x\partial\theta}-(C_{12}^t h_t+C_{33}^t h_t)\frac{\partial^2 v_1}{\partial x\partial\theta}-C_{11}^t h_tR_t\frac{\partial^2 u_1}{\partial x^2}-C_{13}^t h_tR_t\frac{\partial^2 v_1}{\partial x^2}=0 \quad \text{(A1)}$$

$$\frac{G_cR}{h_c}u_2-\frac{G_cR}{h_c}u_1-\frac{C_{23}^b h_b}{R_b}\frac{\partial w}{\partial\theta}-\frac{C_{33}^b h_b}{R_b}\frac{\partial^2 u_2}{\partial\theta^2}-\frac{C_{23}^b h_b}{R_b}\frac{\partial^2 v_2}{\partial\theta^2}-\left(C_{12}^b h_b+G_{xz}R+G_{xz}R\frac{h_b+h_t}{2h_c}\right)\frac{\partial w}{\partial x}$$
$$-2C_{13}^b h_b\frac{\partial^2 u_2}{\partial x\partial\theta}-(C_{12}^b h_b+C_{33}^b h_b)\frac{\partial^2 v_2}{\partial x\partial\theta}-C_{11}^b h_bR_b\frac{\partial^2 u_2}{\partial x^2}-C_{13}^b h_bR_b\frac{\partial^2 v_2}{\partial x^2}=0 \quad \text{(A2)}$$

$$\frac{4R^2-h_c^2}{4h_c^2}G_cLog\left(\frac{2R-h_c}{2R+h_c}\right)v_2+\frac{4Rh_c-4R^2-h_c^2}{4h_c^2}G_cLog\left(\frac{2R-h_c}{2R+h_c}\right)v_1+\left(\frac{1}{8Rh_c^2}(4Rh_c^2+4Rh_ch_t\right.$$
$$\left.+(h_b-h_t)h_c^2-4(h_b+h_t)R^2-8R^2h_c)G_cLog\left(\frac{2R-h_c}{2R+h_c}\right)-\frac{C_{22}^t h_t}{R_t}\right)\frac{\partial w}{\partial\theta}-\frac{C_{23}^t h_t}{R_t}\frac{\partial^2 u_1}{\partial\theta^2}-\frac{C_{22}^t h_t^3}{12R_t^3}\frac{\partial^2 v_1}{\partial\theta^2}$$
$$-\frac{C_{22}^t h_t}{R_t}\frac{\partial^2 v_1}{\partial\theta^2}+\frac{C_{22}^t h_t^3}{12R_t^3}\frac{\partial^3 w}{\partial\theta^3}-C_{23}^t h_t\frac{\partial w}{\partial x}-(C_{12}^t h_t+C_{33}^t h_t)\frac{\partial^2 u_1}{\partial x\partial\theta}-2C_{23}^t h_t\frac{\partial^2 v_1}{\partial x\partial\theta}-\frac{C_{23}^t h_t^3}{6R_t^2}\frac{\partial^2 v_1}{\partial x\partial\theta}+\frac{C_{23}^t h_t^3}{4R_t^2}\frac{\partial^3 w}{\partial x\partial\theta^2}$$
$$-C_{13}^t h_tR_t\frac{\partial^2 u_1}{\partial x^2}-\frac{C_{33}^t h_t^3}{12R_t}\frac{\partial^2 v_1}{\partial x^2}-C_{33}^t h_tR_t\frac{\partial^2 v_1}{\partial x^2}+\frac{C_{12}^t h_t^3}{12R_t}\frac{\partial^3 w}{\partial x^2\partial\theta}+\frac{C_{33}^t h_t^3}{6R_t}\frac{\partial^3 w}{\partial x^2\partial\theta}+\frac{C_{13}^t h_t^3}{12}\frac{\partial^3 w}{\partial x^3}=0 \quad \text{(A3)}$$

$$-\frac{1}{4h_c^2}(4Rh_c+4R^2+h_c^2)G_cLog\left(\frac{2R-h_c}{2R+h_c}\right)v_2+\frac{4R^2-h_c^2}{4h_c^2}G_cLog\left(\frac{2R-h_c}{2R+h_c}\right)v_1+\left(\frac{1}{8Rh_c^2}(4Rh_c^2+4Rh_ch_b\right.$$
$$\left.+(h_b-h_t)h_c^2+4(h_b+h_t)R^2+8R^2h_c)G_cLog\left(\frac{2R-h_c}{2R+h_c}\right)-\frac{C_{22}^b h_b}{R_b}\right)\frac{\partial w}{\partial\theta}-\frac{C_{23}^b h_b}{R_b}\frac{\partial^2 u_2}{\partial\theta^2}-\left(\frac{C_{22}^b h_b^3}{12R_b^3}+\frac{C_{22}^b h_b}{R_b}\right)\frac{\partial^2 v_2}{\partial\theta^2}$$
$$+\frac{C_{22}^b h_b^3}{12R_b^3}\frac{\partial^3 w}{\partial\theta^3}-C_{23}^b h_b\frac{\partial w}{\partial x}-(C_{12}^b h_b+C_{33}^b h_b)\frac{\partial^2 u_2}{\partial x\partial\theta}-\left(2C_{23}^b h_b+\frac{C_{23}^b h_b^3}{6R_b^2}\right)\frac{\partial^2 v_2}{\partial x\partial\theta}+\frac{C_{23}^b h_b^3}{4R_b^2}\frac{\partial^3 w}{\partial x\partial\theta^2}$$
$$-C_{13}^b h_bR_b\frac{\partial^2 u_2}{\partial x^2}-\left(\frac{C_{33}^b h_b^3}{12R_b}+C_{33}^b h_bR_b\right)\frac{\partial^2 v_2}{\partial x^2}+\left(\frac{C_{12}^b h_b^3}{12R_b}+\frac{C_{33}^b h_b^3}{6R_b}\right)\frac{\partial^3 w}{\partial x^2\partial\theta}+\frac{C_{13}^b h_b^3}{12}\frac{\partial^3 w}{\partial x^3}=0 \quad \text{(A4)}$$

$$q_tR_t+q_bR_b+\left(\frac{C_{22}^b h_b}{R_b}+\frac{C_{22}^t h_t}{R_t}\right)w+\frac{C_{23}^b h_b}{R_b}\frac{\partial u_2}{\partial\theta}+\frac{C_{23}^t h_t}{R_t}\frac{\partial u_1}{\partial\theta}$$
$$+\left(\frac{C_{22}^b h_b}{R_b}-\frac{1}{8Rh_c^2}(4Rh_c^2+4Rh_ch_b+(h_b-h_t)h_c^2+4(h_b+h_t)R^2+8R^2h_c)G_cLog\frac{2R-h_c}{2R+h_c}\right)\frac{\partial v_2}{\partial\theta}$$
$$+\left(\frac{C_{22}^t h_t}{R_t}-\frac{1}{8Rh_c^2}(4Rh_c^2+4Rh_ch_t+(h_b-h_t)h_c^2.-4(h_b+h_t)R^2-8R^2h_c)G_cLog\frac{2R-h_c}{2R+h_c}\right)\frac{\partial v_1}{\partial\theta}$$
$$+\left(\frac{1}{16R^2h_c^2}(4R^2+h_c^2)(h_b^2+h_t^2)+\frac{h_c+h_b+h_t}{h_c}+\frac{(4R^2-h_c^2)h_th_b}{8R^2h_c^2}+\frac{2h_c(h_b-h_t)+h_b^2-h_t^2}{4Rh_c}\right)G_c \quad \text{(A5)}$$
$$Log\left(\frac{2R-h_c}{2R+h_c}\right)\frac{\partial^2 w}{\partial\theta^2}-\frac{C_{22}^b h_b^3}{12R_b^3}\frac{\partial^3 v_2}{\partial\theta^3}-\frac{C_{22}^t h_t^3}{12R_t^3}\frac{\partial^3 v_1}{\partial\theta^3}+\left(\frac{C_{22}^b h_b^3}{12R_b^3}+\frac{C_{22}^t h_t^3}{12R_t^3}\right)\frac{\partial^4 w}{\partial\theta^4}+\left(C_{12}^b h_b+G_cR+\frac{G_cR(h_b+h_t)}{2h_c}\right)\frac{\partial u_2}{\partial x}$$
$$+\left(C_{12}^t h_t-G_cR-\frac{G_cR(h_b+h_t)}{2h_c}\right)\frac{\partial u_1}{\partial x}+C_{23}^b h_b\frac{\partial v_2}{\partial x}-\left(\frac{C_{33}^b h_b^3}{6R_b}+\frac{C_{12}^b h_b^3}{12R_b}\right)\frac{\partial^3 v_2}{\partial x^2\partial\theta}+C_{23}^t h_t\frac{\partial v_1}{\partial x}$$
$$-\left(\frac{C_{33}^t h_t^3}{6R_t}+\frac{C_{12}^t h_t^3}{12R_t}\right)\frac{\partial^3 v_1}{\partial x^2\partial\theta}+\left(\frac{C_{33}^b h_b^3}{3R_b}+\frac{C_{33}^t h_t^3}{3R_t}+\frac{C_{12}^b h_b^3}{6R_b}+\frac{C_{12}^t h_t^3}{6R_t}\right)\frac{\partial^4 w}{\partial x^2\partial\theta^2}-\frac{C_{23}^b h_b^3}{4R_b^2}\frac{\partial^3 v_2}{\partial x\partial\theta^2}-\frac{C_{23}^t h_t^3}{4R_t^2}\frac{\partial^3 v_1}{\partial x\partial\theta^2}$$

$$+\left(\frac{C_{23}^{b}h_b^3}{3R_b^2}+\frac{C_{23}^{t}h_t^3}{3R_t^2}\right)\frac{\partial^4 w}{\partial x\partial\theta^3}-\frac{1}{4h_c}(4h_c(h_b+h_c+h_t)+h_b^2+2h_bh_t+h_t^2)G_cR\frac{\partial^2 w}{\partial x^2}$$
$$-\frac{C_{13}^{b}h_b^3}{12}\frac{\partial^3 v_2}{\partial x^3}-\frac{C_{13}^{t}h_t^3}{12}\frac{\partial^3 v_1}{\partial x^3}+\left(\frac{C_{13}^{b}h_b^3}{3}+\frac{C_{13}^{t}h_t^3}{3}\right)\frac{\partial^4 w}{\partial x^3\partial\theta}+\left(\frac{C_{11}^{b}h_b^3R_b}{12}+\frac{C_{11}^{t}h_t^3R_t}{12}\right)\frac{\partial^4 w}{\partial x^4}=0 \quad \text{(A5)}$$

Boundary conditions, on $\theta = 0, \beta$

$$\delta u_1\left\{\frac{C_{23}^{t}h_t}{R_t}w+\frac{C_{33}^{t}h_t}{R_t}\frac{\partial u_1}{\partial\theta}+\frac{C_{23}^{t}h_t}{R_t}\frac{\partial v_1}{\partial\theta}+C_{13}^{t}h_t\frac{\partial u_1}{\partial x}+C_{33}^{t}h_t\frac{\partial v_1}{\partial x}\right\}=0 \quad \text{(A6)}$$

$$\delta u_2\left\{\frac{C_{23}^{b}h_b}{R_b}w+\frac{C_{33}^{b}h_b}{R_b}\frac{\partial u_2}{\partial\theta}+\frac{C_{23}^{b}h_b}{R_b}\frac{\partial v_2}{\partial\theta}+C_{13}^{b}h_b\frac{\partial u_2}{\partial x}+C_{33}^{b}h_b\frac{\partial v_2}{\partial x}\right\}=0 \quad \text{(A7)}$$

$$\delta v_1\left\{\frac{C_{22}^{t}h_t}{R_t}w+\frac{C_{23}^{t}h_t}{R_t}\frac{\partial u_1}{\partial\theta}+\left(\frac{C_{22}^{t}h_t^3}{12R_t^3}+\frac{C_{22}^{t}h_t}{R_t}\right)\frac{\partial v_1}{\partial\theta}-\frac{C_{22}^{t}h_t^3}{12R_t^3}\frac{\partial^2 w}{\partial\theta^2}\right.$$
$$\left.+C_{12}^{t}h_t\frac{\partial u_1}{\partial x}+\left(C_{23}^{t}h_t+\frac{C_{23}^{t}h_t^3}{12R_t^2}\right)\frac{\partial v_1}{\partial x}-\frac{C_{23}^{t}h_t^3}{6R_t^2}\frac{\partial^2 w}{\partial x\partial\theta}-\frac{C_{12}^{t}h_t^3}{12R_t}\frac{\partial^2 w}{\partial x^2}\right\}=0 \quad \text{(A8)}$$

$$\delta v_2\left\{\frac{C_{22}^{b}h_b}{R_b}w+\frac{C_{23}^{b}h_b}{R_b}\frac{\partial u_2}{\partial\theta}+\left(\frac{C_{22}^{b}h_b^3}{12R_b^3}+\frac{C_{22}^{b}h_b}{R_b}\right)\frac{\partial v_2}{\partial\theta}-\frac{C_{22}^{b}h_b^3}{12R_b^3}\frac{\partial^2 w}{\partial\theta^2}\right.$$
$$\left.+C_{12}^{b}h_b\frac{\partial u_2}{\partial x}+\left(C_{23}^{b}h_b+\frac{C_{23}^{b}h_b^3}{12R_b^2}\right)\frac{\partial v_2}{\partial x}-\frac{C_{23}^{b}h_b^3}{6R_b^2}\frac{\partial^2 w}{\partial x\partial\theta}-\frac{C_{12}^{b}h_b^3}{12R_b}\frac{\partial^2 w}{\partial x^2}\right\}=0 \quad \text{(A9)}$$

$$\delta w\left\{\frac{1}{16h_c^2R^2}G_c(h_c(h_b-h_t)+2(h_b+2h_c+h_t)R)Log\left(\frac{2R-h_c}{2R+h_c}\right)\left(2R(h_c+2R)v_2+2R(h_c-2R)v_1-\right.\right.$$
$$\left.-(h_c(h_b-h_t)+2(h_b+2h_c+h_t)R)\frac{\partial w}{\partial\theta}\right)+\frac{C_{22}^{b}h_b^3}{12R_b^3}\frac{\partial^2 v_2}{\partial\theta^2}+\frac{C_{22}^{t}h_t^3}{12R_t^3}\frac{\partial^2 v_1}{\partial\theta^2}-\left(\frac{C_{22}^{b}h_b^3}{12R_b^3}+\frac{C_{22}^{t}h_t^3}{12R_t^3}\right)\frac{\partial^3 w}{\partial\theta^3}+\frac{C_{23}^{b}h_b^3}{4R_b^2}\frac{\partial^2 v_2}{\partial x\partial\theta}$$
$$+\frac{C_{23}^{t}h_t^3}{4R_t^2}\frac{\partial^2 v_1}{\partial x\partial\theta}-\left(\frac{C_{23}^{b}h_b^3}{3R_b^2}+\frac{C_{23}^{t}h_t^3}{3R_t^2}\right)\frac{\partial^3 w}{\partial x\partial\theta^2}+\frac{C_{33}^{b}h_b^3}{6R_b}\frac{\partial^2 v_2}{\partial x^2}+\frac{C_{33}^{t}h_t^3}{6R_t}\frac{\partial^2 v_1}{\partial x^2}$$
$$\left.-\left(\frac{C_{12}^{b}h_b^3}{12R_b}+\frac{C_{33}^{b}h_b^3}{3R_b}+\frac{C_{12}^{t}h_t^3}{12R_t}+\frac{C_{33}^{t}h_t^3}{3R_t}\right)\frac{\partial^3 w}{\partial x^2\partial\theta}-\left(\frac{C_{13}^{b}h_b^3}{6}+\frac{C_{13}^{t}h_t^3}{6}\right)\frac{\partial^3 w}{\partial x^3}\right\}=0 \quad \text{(A10)}$$

$$\delta\frac{\partial w}{\partial\theta}\left\{-\frac{C_{22}^{b}h_b^3}{12R_b^3}\frac{\partial v_2}{\partial\theta}-\frac{C_{22}^{t}h_t^3}{12R_t^3}\frac{\partial v_1}{\partial\theta}+\left(\frac{C_{22}^{b}h_b^3}{12R_b^3}+\frac{C_{22}^{t}h_t^3}{12R_t^3}\right)\frac{\partial^2 w}{\partial\theta^2}\right.$$
$$\left.-\frac{C_{23}^{b}h_b^3}{12R_b^2}\frac{\partial v_2}{\partial x}-\frac{C_{23}^{t}h_t^3}{12R_t^2}\frac{\partial v_1}{\partial x}+\left(\frac{C_{23}^{b}h_b^3}{6R_b^2}+\frac{C_{23}^{t}h_t^3}{6R_t^2}\right)\frac{\partial^2 w}{\partial x\partial\theta}+\left(\frac{C_{12}^{b}h_b^3}{12R_b}+\frac{C_{12}^{t}h_t^3}{12R_t}\right)\frac{\partial^2 w}{\partial x^2}\right\}=0 \quad \text{(A11)}$$

Note that in addition to above equations, for considered boundary conditions, some other relations must be implemented, as following:

Clamped (C):

$$\delta u_1=\delta u_2=\delta v_1=\delta v_2=\delta w=\delta\frac{\partial w}{\partial\theta}=0$$

Simply supported (S):

$$\delta u_1=\delta u_2=\delta w=0;\ \delta v_1\neq 0;\ \delta v_2\neq 0;\ \delta\frac{\partial w}{\partial\theta}\neq 0$$

Free (F):

$$\delta u_1\neq 0; \delta u_2\neq 0; \delta w\neq 0;\ \delta v_1\neq 0;\ \delta v_2\neq 0;\ \delta\frac{\partial w}{\partial\theta}\neq 0$$

Boundary conditions, on $x = 0, L$

$$-\frac{C_{23}^{b}h_b^3}{12R_b^2}\frac{\partial v_2}{\partial x}-\frac{C_{23}^{t}h_t^3}{12R_t^2}\frac{\partial v_1}{\partial x}+\left(\frac{C_{23}^{b}h_b^3}{6R_b^2}+\frac{C_{23}^{t}h_t^3}{6R_t^2}\right)\frac{\partial^2 w}{\partial x\partial\theta}+\left(\frac{C_{12}^{b}h_b^3}{12R_b}+\frac{C_{12}^{t}h_t^3}{12R_t}\right)\frac{\partial^2 w}{\partial x^2}\Bigg\} \tag{A12}$$

$$\delta u_2\left\{C_{12}^{b}h_b w+C_{13}^{b}h_b\frac{\partial u_2}{\partial\theta}+C_{12}^{b}h_b\frac{\partial v_2}{\partial\theta}+C_{11}^{b}h_bR_b\frac{\partial u_2}{\partial x}+C_{13}^{b}h_bR_b\frac{\partial v_2}{\partial x}\right\}=0 \tag{A13}$$

$$\begin{aligned}&\delta v_1\Bigg\{C_{23}^{t}h_t w+C_{33}^{t}h_t\frac{\partial u_1}{\partial\theta}+\left(\frac{C_{23}^{t}h_t^3}{12R_t^2}+C_{23}^{t}h_t\right)\frac{\partial v_1}{\partial\theta}-\frac{C_{23}^{t}h_t^3}{12R_t^2}\frac{\partial^2 w}{\partial\theta^2}\\&+C_{13}^{t}h_tR_t\frac{\partial u_1}{\partial x}+\left(C_{33}^{t}h_tR_t+\frac{C_{33}^{t}h_t^3}{12R_t}\right)\frac{\partial v_1}{\partial x}-\frac{C_{33}^{t}h_t^3}{6R_t}\frac{\partial^2 w}{\partial x\partial\theta}-\frac{C_{13}^{t}h_t^3}{12}\frac{\partial^2 w}{\partial x^2}\Bigg\}=0\end{aligned} \tag{A14}$$

$$\begin{aligned}&\delta v_2\Bigg\{C_{23}^{b}h_b w+C_{33}^{b}h_b\frac{\partial u_2}{\partial\theta}+\left(\frac{C_{23}^{b}h_b^3}{12R_b^2}+C_{23}^{b}h_b\right)\frac{\partial v_2}{\partial\theta}-\frac{C_{23}^{b}h_b^3}{12R_b^2}\frac{\partial^2 w}{\partial\theta^2}\\&+C_{13}^{b}h_bR_b\frac{\partial u_2}{\partial x}+\left(C_{33}^{b}h_bR_b+\frac{C_{33}^{b}h_b^3}{12R_b}\right)\frac{\partial v_2}{\partial x}-\frac{C_{33}^{b}h_b^3}{6R_b}\frac{\partial^2 w}{\partial x\partial\theta}-\frac{C_{13}^{b}h_b^3}{12}\frac{\partial^2 w}{\partial x^2}\Bigg\}=0\end{aligned} \tag{A15}$$

$$\begin{aligned}&\delta w\Bigg\{\frac{C_{23}^{b}h_b^3}{6R_b^2}\frac{\partial^2 v_2}{\partial\theta^2}+\frac{C_{23}^{t}h_t^3}{6R_t^2}\frac{\partial^2 v_1}{\partial\theta^2}-\left(\frac{C_{23}^{b}h_b^3}{6R_b^2}+\frac{C_{23}^{t}h_t^3}{6R_t^2}\right)\frac{\partial^3 w}{\partial\theta^3}+\frac{G_c(h_b+2h_c+h_t)R}{4h_c}\left(-2u_2+2u_1+(h_b+2h_c+h_t)\frac{\partial w}{\partial x}\right)\\&+\left(\frac{C_{12}^{b}h_b^3}{12R_b}+\frac{C_{33}^{b}h_b^3}{6R_b}\right)\frac{\partial^2 v_2}{\partial x\partial\theta}+\left(\frac{C_{12}^{t}h_t^3}{12R_t}+\frac{C_{33}^{t}h_t^3}{6R_t}\right)\frac{\partial^2 v_1}{\partial x\partial\theta}-\left(\frac{C_{12}^{b}h_b^3}{12R_b}+\frac{C_{33}^{b}h_b^3}{3R_b}+\frac{C_{12}^{t}h_t^3}{12R_t}+\frac{C_{33}^{t}h_t^3}{3R_t}\right)\frac{\partial^3 w}{\partial x\partial\theta^2}\\&+\frac{C_{13}^{b}h_b^3}{12}\frac{\partial^2 v_2}{\partial x^2}+\frac{C_{13}^{t}h_t^3}{12}\frac{\partial^2 v_1}{\partial x^2}-\left(\frac{C_{13}^{b}h_b^3}{3}+\frac{C_{13}^{t}h_t^3}{3}\right)\frac{\partial^3 w}{\partial x^2\partial\theta}-\left(\frac{C_{11}^{b}h_b^3R_b}{12}+\frac{C_{11}^{t}h_t^3R_t}{6}\right)\frac{\partial^3 w}{\partial x^3}\Bigg\}=0\end{aligned} \tag{A16}$$

$$\begin{aligned}&\delta\frac{\partial w}{\partial x}\Bigg\{-\frac{C_{12}^{b}h_b^3}{12R_b}\frac{\partial v_2}{\partial\theta}-\frac{C_{12}^{t}h_t^3}{12R_t}\frac{\partial v_1}{\partial\theta}+\left(\frac{C_{12}^{b}h_b^3}{12R_b}+\frac{C_{12}^{t}h_t^3}{12R_t}\right)\frac{\partial^2 w}{\partial\theta^2}-\frac{C_{13}^{b}h_b^3}{12}\frac{\partial v_2}{\partial x}-\frac{C_{13}^{t}h_t^3}{12}\frac{\partial v_1}{\partial x}\\&+\left(\frac{C_{13}^{b}h_b^3}{6}+\frac{C_{13}^{t}h_t^3}{6}\right)\frac{\partial^2 w}{\partial x\partial\theta}+\left(\frac{C_{11}^{b}h_b^3R_b}{12}+\frac{C_{11}^{t}h_t^3R_t}{12}\right)\frac{\partial^2 w}{\partial x^2}\Bigg\}=0\end{aligned} \tag{A17}$$

Note that in addition to above equations, for considered boundary conditions, some other relations must be implemented, as following:

Clamped (C):

$$\delta u_1=\delta u_2=\delta v_1=\delta v_2=\delta w=\delta\frac{\partial w}{\partial x}=0$$

Simply supported (S):

$$\delta v_1=\delta v_2=\delta w=0;\ \delta u_1\neq 0;\ \delta u_2\neq 0;\ \delta\frac{\partial w}{\partial x}\neq 0$$

Free (F):

$$\delta u_1\neq 0;\delta u_2\neq 0;\delta w\neq 0;\ \delta v_1\neq 0;\ \delta v_2\neq 0;\ \delta\frac{\partial w}{\partial x}\neq 0$$

Appendix B

Discretized form of Equation (A1)

$$\begin{aligned}&-\frac{G_cR}{h_c}u_{2_{i,j}}+\frac{G_cR}{h_c}u_{1_{i,j}}-\frac{C_{23}^{t}h_t}{R_t}\sum_{l=1}^{N_\theta}B_{jl}^{(1)}w_{i,l}-\frac{C_{33}^{t}h_t}{R_t}\sum_{l=1}^{N_\theta}B_{jl}^{(2)}u_{1_{i,l}}-\frac{C_{23}^{t}h_t}{R_t}\sum_{l=1}^{N_\theta}B_{jl}^{(2)}v_{1_{i,l}}\\&+\left(-C_{12}^{t}h_t+G_cR\frac{h_b+2h_c+h_t}{2h_c}\right)\sum_{k=1}^{N_x}A_{ik}^{(1)}w_{k,j}-2C_{13}^{t}h_t\sum_{k=1}^{N_x}\sum_{l=1}^{N_\theta}A_{ik}^{(1)}B_{jl}^{(1)}u_{1_{k,l}}\\&-(C_{12}^{t}h_t+C_{33}^{t}h_t)\sum_{k=1}^{N_x}\sum_{l=1}^{N_\theta}A_{ik}^{(1)}B_{jl}^{(1)}v_{1_{k,l}}-C_{11}^{t}h_tR_t\sum_{k=1}^{N_x}A_{ik}^{(2)}u_{1_{k,j}}-C_{13}^{t}h_tR_t\sum_{k=1}^{N_x}A_{ik}^{(2)}v_{1_{k,j}}=0\end{aligned} \tag{B1}$$